Angular Momentum in Ion-Molecule Reactions

G. G. Meisels,* G. M. L. Verboom, M. J. Weiss, and TaCheng Hsieh

Contribution from the Department of Chemistry, University of Nebraska, Lincoln, Nebraska 68588. *Received November 3, 1978*

Abstract: The fragmentation of gaseous ions is described using a formalism based on RRKM and a joint distribution function of energy and angular momentum $P(E,J)$; it is particularly suitable for the study of angular momentum effects, and is tested by evaluating the branching ratio for the competitive fragmentation pathways of an intermediate complex prepared in different rotational distributions with nearly identical total internal energy. The model is applied to the fragmentation of $C_4H_8^+$ to $C_4H_7^+$ (k_1) and $C_3H_5^+$ (k_2) and compared with experiment. When $C_4H_8^+$ is prepared by the condensation of ethylene ion and ethylene, $k_1/k_2 \sim 0.11$. When $C_4H_8^+$ is produced by photoionization of neutral C_4H_8 olefins at a fixed internal energy corresponding to the heat of reaction of the condensation process, by using threshold photoelectron-coincident photoion mass spectrometry, $k_1/k_2 \sim 0.39$. Angular momentum clearly has a major effect on the relative contributions of competing reaction exit channels, particularly when one pathway leads to fragments with low reduced mass and polarizability. The possible neglect or inclusion of rotational energy and/or rotational angular momentum of the reactants in $P(E,J)$ and $k(E,J)$ leads to three different predictions, which increasingly emphasize the effect of angular momentum on the reaction outcome. Agreement between theory and experiment is satisfactory.

Introduction

Angular momentum is a parameter of considerable current interest in studies of state-to-state chemistry.[1] It is well known from molecular beam studies of neutral-neutral reactions[2] that the angular momentum resulting from the collision process manifests itself in the angular and velocity distributions of the receding products. In ion-neutral reactions, the long-range attractive forces lead to even larger angular momentum effects.[3] In macroscopic systems such as those of interest to gas-phase chemists one is concerned with lifetimes, overall reaction rates, and the relative probability of fragmentation of a transient complex when several channels are available. The role of angular momentum in affecting these quantities is not clear. Early investigators[4] recognized that the exit channel is constrained by the conservation of angular momentum. Phase space theory addressed this aspect clearly[5] but ignored the nature of the intermediate ion. This approach has recently experienced significant development by Klots[6] and by Chesnavich and Bowers,[7] with considerable success. Transition-state models based upon RRKM, without rigorous conservation of angular momentum, have also been employed with varying success;[8,9] these have assumed a loose transition state and are therefore formally equivalent to phase space theory.[10]

Little definitive experimental evidence exists. Early surveys noted the similarity of the distribution of the products when the same intermediate was prepared by collision and by electron impact from the molecular analogue.[11] Since the angular momentum distributions of species formed by collision or direct ionization should differ considerably, it suggested that angular momentum plays a minor role. Kinetic energy release measurements[12] clearly made the distinction; these may be interpreted in terms of phase space theory[6,12] or in terms of a recent reformulation of RRKM which accounts for these and other energy disposal measurements.[13]

It is of particular interest to uncover whether angular momentum can significantly alter overall product distributions, that is, whether it really affects the net chemistry observed in a given system. Such effects can certainly be expected to be largest where one of the reactions paths is loss of a hydrogen atom. It is precisely in such fragmentations that transition-state theory has in the past found it necessary to employ tight transition states to obtain agreement with experiment;[14] this suggests that models based purely on phase space arguments, which neglect the nature and effect of the critical reaction complex, may be inadequate. We have therefore chosen to develop a model and a formalism based on RRKM theory which we believe to be particularly suitable for the study of angular momentum effects. Our approach is in several ways similar to one reported earlier by Waage and Rabinovitch,[15] but differs in the form through which it takes account of energy and angular momentum distributions. While we apply it here to the evaluation of branching ratios of competitive fragmentation pathways, in accord with our interest in the effect of angular momentum on the overall reaction chemistry, our approach may also be modified readily to calculate other parameters. We test our model with the fragmentation of $C_4H_8^+$ prepared in two distributions of rotational states but with nearly identical total internal energy.

Experimental Section

The threshold photoelectron-coincident photoion mass spectrometer employed in these studies has been described elsewhere.[16,17] The apparatus uses a 1-m normal incidence vacuum ultraviolet monochromator with a light source producing the Hopfield continuum in helium. The resolution of the monochromator was set at 0.04 nm. Wavelength-selected light enters an ionization chamber, one side of which consists of a collimated hole structure which rejects the passage of energetic electrons. Near-thermal electrons passing through this stearadiancy energy analyzer are detected by a channeltron electron multiplier, which provides the start pulse for a time to pulse height converter (TTPHC). Ions are extracted in the opposite direction by the weak field (ca. 10 V cm^{-1}), mass selected in an Extranuclear 4-324-9 quadrupole mass filter if necessary, and detected using a second channeltron multiplier. The pulse generated by the ion terminates the TTPHC, which creates a pulse whose height is proportional to the ion flight time. These pulses are sorted using a multichannel pulse height analyzer, yielding a time-of-flight mass spectrum of only those ions formed in coincidence with zero kinetic energy electrons. The overall energy resolution of the instrument was 0.020 eV fwhm as measured by examining the ionization of argon at threshold.

The fragment ion distributions at an internal energy of 2.57 eV with respect to the most stable 2-butene ion structure[18,19] were obtained at a calibrated photon energy of 11.69 eV from both *trans*-2-butene and *cis*-2-butene. Spectra were initially obtained using time-of-flight mass separation only at a resolution of about $m/\Delta m = 25$, and later verified by mass selection using the quadrupole mass filter at a resolution of 70.

The Model

Our point of departure is based on distribution functions of $P(E,J)$ in total energy E and total angular momentum J, coupled with established methodology[18] to describe a microscopic rate constant $k(E,J)$ explicitly in terms of energy and angular momentum only, with temperature entering princi-

0002-7863/79/1501-7189$01.00/0

pally through $P(E,J)$:

$$k(E,J) = \frac{pG^*(E - E_0)}{hN(E_n)} \qquad E - E_0 > 0 \qquad \text{(I)}$$

where E and J are the total energy and angular momentum, and are constants of motion. G^* is the sum of states at the transition state, N is the density of states of the ionic complex, p is the ratio of symmetry numbers (path degeneracy), h is Planck's constant, E_0 is the threshold energy of the reaction, and E_n is the total randomizable energy available in the complex. The microscopic rate constant $k(T)$ is obtained by multiplication of (I) by the joint distribution function $P(E,J)$ and integration over the appropriate limits of E and J. Then

$$k(T) = \iint k(E,J)P(E,J)\,\mathrm{d}J\,\mathrm{d}E \qquad \text{(II)}$$

where the ranges of the integrations are either $E = E(J)$, ∞ and $J = 0$, ∞ or $J = J(E)$, ∞ and $E = 0$, ∞ depending upon the order in which the integrations of eq II are performed. $E(J)$ and $J(E)$ are the limiting values for which a complex is formed at constant J and E, respectively. As discussed below, our approach is restricted to systems where spherically symmetric long-range forces describe adequately the interaction between the separated partners or products of the collision.

Before we proceed to define $P(E,J)$ and $k(E,J)$, we choose a system amenable to experimental test on which to perform model calculations. We have selected the fragmentation of $C_4H_8^+$ for this purpose because it can be prepared with at least two different rotational angular momentum distributions by photoionization and by collision:

$$C_4H_8 \xrightarrow[-e]{h\nu} (C_4H_8^+)^*$$

$$C_2H_4^+ + C_2H_4 \rightarrow (C_4H_8)^*$$

and because it fragments principally via reactions 1 and 2.

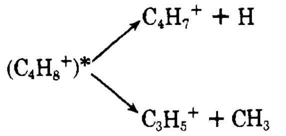

$$(C_4H_8^+)^* \rightarrow C_4H_7^+ + H \qquad (1)$$

$$(C_4H_8^+)^* \rightarrow C_3H_5^+ + CH_3 \qquad (2)$$

Reaction 1 is thought to proceed via a tight transition state; the small reduced mass of the fragments and the low polarizability of H should make this reaction particularly sensitive to angular momentum.

We continue to develop our model by examining the branching ratio for two competitive pathways arising from a common ionic complex but from two different transition states, (1) and (2). This is simply

$$\frac{k_1}{k_2}(E,J) = \frac{p_1G_1^*(E - E_{0,1})}{p_2G_2^*(E - E_{0,2})} \qquad \text{(III)}$$

where now $E - E_{0,1}$ and $E - E_{0,2}$ are the excess energies available for randomization in the transition state for reactions 1 and 2, respectively. The observable branching ratio is obtained by averaging k_1/k_2 using the distribution function $P(E,J)$, that is

$$\langle k_1/k_2 \rangle = \int_J \int_E (k_1/k_2)(E,J)P(E,J)\,\mathrm{d}E\,\mathrm{d}J \qquad \text{(IV)}$$

This introduces a minor error which does not significantly affect our results.[20]

The above expression has two components. The first is $P(E,J)$; it is determined by the method of preparation of the molecular ion. The second is k_1/k_2; it is an inherent property of the complex, and defined by E and J. Angular momentum will play a role as long as k_1/k_2 (E,J), the microcanonical branching ratio, depends strongly on $E - E_0$, the energy available for randomization in the transition state. This quantity may be expressed as

$$E - E_0 = E - V_{\mathrm{eff},t} - E_{0,\mathrm{fragment}} \qquad \text{(Va)}$$

where E is the total energy of the system, $E_{0,\mathrm{fragment}}$ is the reference energy of the potential (the energy of the fragments at infinite separation), and $V_{\mathrm{eff},t}$ is the maximum in the effective potential along the dissociative reaction coordinate (Figure 1).

If the fragmentation is treated in the quasi-diatomic approximation, and the attractive potential is defined entirely by ion-induced dipole forces, one obtains

$$V_{\mathrm{eff}} = \frac{J^2}{2\mu r^2} - \frac{\alpha e^2}{2r^4} \qquad \text{(VIa)}$$

Substitution of r_t obtained by setting $\mathrm{d}V_{\mathrm{eff}}/\mathrm{d}r = 0$ leads to

$$V_{\mathrm{eff},t} = J^4/8\alpha e^2\mu^2 \qquad \text{(VIb)}$$

Here α is the polarizability of the neutral fragment, μ is the reduced mass of the fragments, and r_t is the location of the transition state. It bears emphasis that within the quasi-diatomic approximation, and only then, eq Va reduces to

$$E - E_0 = E - E_{0,\mathrm{fragment}} - J^4/(8\alpha e^2\mu^2) \qquad \text{(Vb)}$$

The last expression indicates that low polarizability and low reduced mass will increase the barrier and, therefore, emphasize the effect of angular momentum.

The last term in (Vb) defines the barrier toward dissociation. One may ask to what extent rotation of the departing fragments will cause a difference between L_{exit} and J. The major assumption in this approach is neglect of rotation about the axis connecting fragments. Since rotation of the departing species may add or subtract from J to give L, the average L should be approximately equal to J. Moreover, and particularly for a tight complex, conversion of the bending mode to a rotation should certainly lead to rotation in opposite directions, largely canceling out the contribution of product rotation to the overall angular momentum. The condition that the interaction potential be spherically symmetrical is much less stringent. This may be of some difficulty for reactions such as (1) where reduced mass and polarizability of the neutral are low, the transition state is tight, and r_t is close in. When the transition state is loose and the overwhelming number of reactions occur at values of r_t quite large in comparison to molecular dimensions[3] (Vb) should be a good representation.

An estimated energy surface for reaction 2 at $J = 140\hbar$ is shown in Figure 1; it is approximately to scale. In order to make the surface more realistic, a repulsive term of the form $V_r = Ar^{-12}$ was added. The coefficient A was determined by forcing the minimum to correspond to the assumed dissociation limit of 18 000 $\mathrm{cm^{-1}}$. This resulted in a bond distance $r_0 = 0.147$ nm, reasonably close to typical C–H bond lengths of 0.153 nm. The location of the transition state is 0.291 nm at this value of J; r_t is always large enough that the repulsive potential does not affect it. The total energy E_n of the system is the sum of the heat of reaction and the thermal energy of 2-butene ion.

The System

The system we have chosen for this study is the fragmentation of $C_4H_8^+$ which dissociates mainly via (1) and (2) at internal energies of interest here. It is necessary to review briefly the justification for using the same basic parameters to describe the $C_4H_8^+$ ions produced with different angular momentum distributions either by condensation of ethylene ion and ethylene or by photoionization of one of the butene isomers such as *trans*-2-butene.

It was established very early through charge-exchange experiments in closed systems that $C_4H_8^+$ prepared as a collision

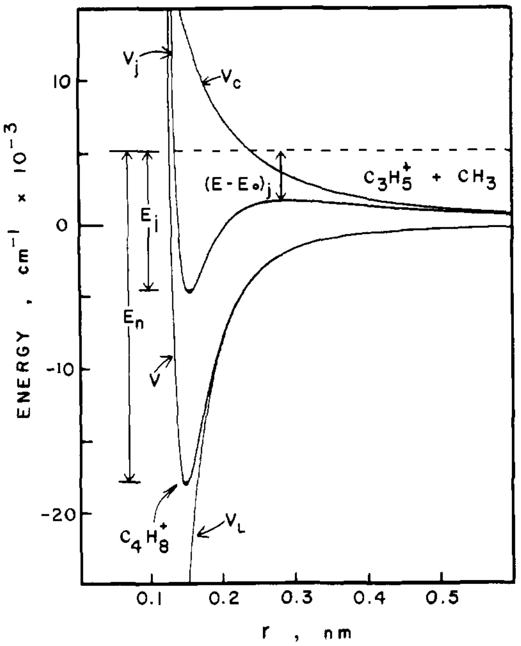

Figure 1. Energy surface for fragmentation of $C_4H_8^+$ to $C_3H_5^+$ and CH_3. The potentials shown include the centrifugal potential $V_c = J^2/2\mu r^2$, the polarization attraction $V_L = \alpha e^2/2r^4$, and the total potentials V and V_J including a repulsive term $V_r = 9.54 \times 10^{-7} r^{-12}$ The curve for zero angular momentum is designated V and that for $J = 140\hbar$ is indicated by V_J. E_n is the total energy of 2-butene ion formed by the collision process; it is also the total randomizable energy when $J = 0$. E_J is the total randomizable energy of $C_4H_8^+$ and $(E - E_0)_J$ is the nonfixed, random excess energy in the transition state when $J = 140\hbar$.

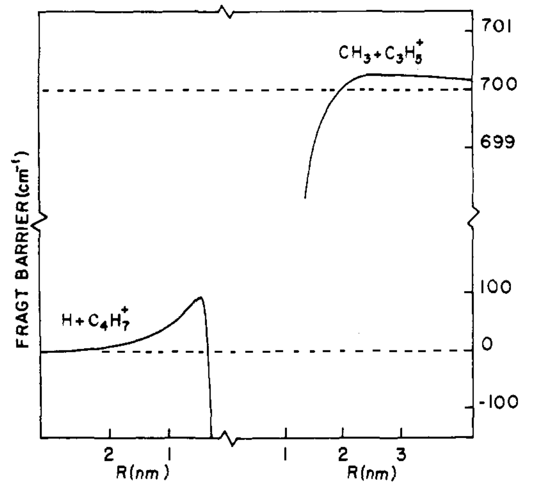

Figure 2. Representative surface for fragmentation of $C_4H_8^+$ at $J = 15\hbar$; note the difference in energy scales.

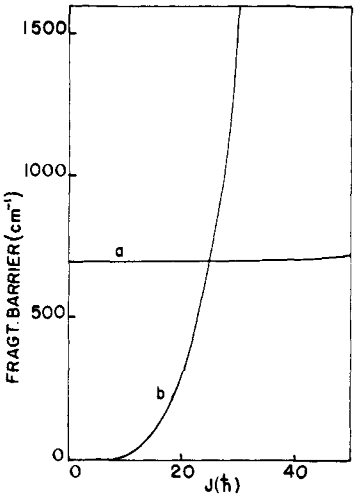

Figure 3. Effect of angular momentum on fragmentation barrier: (a) reaction 2; (b) reaction 1.

adduct has a lifetime on the order of 10^{-7} s and that the neutral product of the electron transfer had the 2-butene and 2-methylpropene structures.[22] Later studies using beam techniques showed that the angular distributions of the products of reaction 1 and 2 are isotropic.[23] Deuterium and ^{13}C labeling of butenes prior to ionization[24,25] confirmed earlier findings[26] that ionization is followed by extensive randomization of hydrogen atoms and that skeletal rearrangement takes place at internal energies of the molecular ion in excess of fragmentation thresholds. This is further confirmed by recent studies[27,28] which demonstrate that the identity of the neutral olefinic precursor does not affect the fragmentation process (2) provided that the internal energies relative to the most stable ionic structure are the same for each isomer. The support for a commonality of structures of the $C_4H_8^+$ formed by collision and by photoionization is overwhelming, and the demonstrated long lifetime of the complex establishes the applicability of statistical theories.

The Transition State

It is customary to employ a unique transition state for each fragmentation pathway.[8,9,13,14,21] This is indeed applicable when all fragmentations occur on the same surface, but this is clearly not the case when there is a large distribution of angular momenta so that a wide distribution of values r_t and $E - E_0$ exists.[3] In reality there is an infinite number of transition states defined by the range of values of r_t. In principle, therefore, one should define the properties of the transition state separately for each value of r_t. Fortunately, simplifications are possible. For most dissociations the majority of values of r_t are at separations large enough to permit neglect of interaction between the separating species so that a loose transition state is applicable. This description becomes equivalent to phase space theory and permits definition of a singular set of frequencies for the transition state, essentially very similar to the product species, with little error. This is the case for reaction 2. The matter is more complicated when a tight transition state must be involved. In our system, this is the case for reaction 1, but a single transition state may still be retained as a result of the weak attraction between the separating partners. A representative potential energy surface at $J = 15\hbar$ (Figure 2) demonstrates that, even for small values of the angular momentum, the repulsive part of the effective potential leads to a steep, close-in barrier which does not move greatly as J is increased to the limit where the rotational barrier prevents fragmentation in that direction. As all such barriers, r decreases with increasing values of J. The relatively small range of values of r_t which results permits the assignment of a unique set of frequencies for the transition state. The distribution of transition states in both cases is taken into account in terms of the barrier height so that an infinite number of transition states is retained within this limited sense.

It is interesting to examine the manifestations of differences in mass and polarizabilities on the barriers associated with reactions 1 and 2; this is dramatically demonstrated in Figure 3, which shows the weak variation of the barrier toward reaction 2 with L, in sharp contrast to the steep rise of the barrier toward reaction 1 at values of L in excess of about $20\hbar$. It is immediately clear that the calculated branching ratio must reflect this dependence of the barrier on angular momentum.

Our calculations were carried out using only two sets of frequencies derived from 1-butene by making simple changes

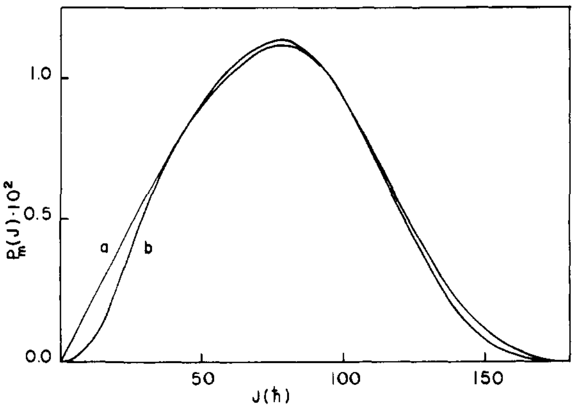

Figure 4. $P_c(J)$ with (a) and without (b) neglect of reactant rotations at 300 K.

Table I. Parameters Used in the Calculation for Formation and Fragmentation of $C_4H_8^+$

	$C_3H_5^+$-CH_3	$C_4H_7^+$-H	$C_2H_4^+$-C_2H_4
polarizability, Å^3	2.2	0.667	4.22
reduced mass, amu	11.0	0.98	14.0
$B_1 = B_2$			1.588
barrier, cm^{-1} [a]	18 000	17 300	
path degeneracy	1	2	
frequencies[b] (deg[c])		200 (1)	
	300 (2)		
	400 (1)	400 (1)	
		600 (2)	
	700 (3)	700 (4)	
	725 (2)		
	800 (1)	800 (1)	
	900 (2)	900 (2)	
	1000 (1)	1000 (2)	
	1200 (2)	1200 (2)	
	1300 (2)	1300 (2)	
	1350 (1)	1350 (1)	
	1400 (1)		
	1450 (2)	1450 (2)	
		2175 (2)	
	2950 (8)	2950 (7)	
rotations[b] (deg[c])	5.92 (1)		

[a] The energy barrier is given with respect to the *cis*-2-butene ion. [b] Frequencies are given in cm^{-1}. [c] Degeneracy.

following established guidelines[29,30] (Table I). Our description of the transition state is consistent with an analysis of Lossing, based on heats of formation and appearance potentials; these indicate that methylallyl ion and allyl ion are the most likely structures for the product ions.[27] The fragmentation barrier at zero angular momentum and infinite separation for reaction 2 was taken from the appearance potential measurements of Lossing, while the value for hydrogen loss (reaction 1) was adjusted for best fit of the experimental fragmentation of methylcyclopropane ion at an internal energy of 3.78 eV with respect to *trans*-2-butene ion; it is within the error limits of experimental evaluations.

The Distribution Function $P(E,J)$

The preparation of $C_4H_8^+$ by condensation of C_2H_4 and $C_2H_4^+$, and by threshold photoelectron coincident photoion mass spectrometry, generates different distributions of energies and angular momenta. We assume that precursors are in their ground electronic states and in thermal equilibrium. The initial vibrational energy is taken into account by including the average thermal energy stored in the vibrational modes of the reactants in the total energy of the system. The evaluation of $P(E,J)$ then reduces to finding, for the transient complex, the distribution of the initial relative translational and/or rotational parameters that describe the precursors.

A. Collision Process. The Hamiltonian describing the collision is assumed to be separable into its components

$$H = H_t + H_{r1} + H_{r2}$$

where the subscripts r and t signify rotation and relative translation. We have already discussed the angular momentum distribution in the case where the rotational properties of the reactant molecules are ignored, i.e., where J is simply replaced by L, the orbital angular momentum arising from the collision process.[3] The joint distribution function in terms of the initial relative kinetic energy ϵ_t is

$$P_c(\epsilon_t,L) = \frac{2\sqrt{2\pi}\hbar^2}{k_L(\mu KT)^{3/2}} L \exp\left(-\frac{\epsilon_t}{kT}\right)$$

$$\epsilon_t > L^4/\Lambda$$

$$\Lambda = 8\alpha e^2\mu^2/\hbar^4 \qquad \text{(VII)}$$

where $k_L = 2\pi e\sqrt{\alpha/\mu}$, the Langevin capture rate constant, and the inequality condition must be met for complex formation.

Allowance for rotational distribution of the reactants can be made in closed form if both reactants are assumed to be spherical (see Appendix I) and leads to

$$P_{c,s}(\epsilon_{tr},J) = \frac{8}{15}\sqrt{\frac{2B_r}{\pi}}\frac{\hbar^2}{k_L(\mu kT)^{3/2}} \times \frac{J}{(kT)^3} - \exp\left(-\frac{\epsilon_{tr}}{kT}\right) F(\epsilon_{tr},J) \qquad \text{(VIII)}$$

where

$$F(\epsilon_{tr},J) = \int_{L-}^{L+} [z^* - B_r(J-L)^2]^{5/2}\,dL$$

for

$$\epsilon_{tr}(J) \leqslant \epsilon_{tr} \leqslant B_rJ^2$$

and

$$F(\epsilon_{tr},J) = \int_0^{L+} [z^* - B_r(J-L)^2]^{5/2}\,dL - \int_0^{L-} [z^* - B_r(J+L)^2]^{5/2}\,dL \qquad \text{(IX)}$$

for

$$B_rJ^2 \leqslant \epsilon_{tr}$$

with

$$z^* = \epsilon_{tr} - L^4/\Lambda$$

where now ϵ_{tr} is the sum of the initial rotational and translational energies and B_r is the reduced rotational constant of the reactants. L^+ and L^- are the intersection of the energy and angular momentum boundaries in the L, J_r plane.[7b,13] Here, again, a particular momentum state of the complex cannot be formed unless the energy is in excess of a value that depends upon the angular momentum.

It is instructive to examine the resulting distributions of angular momenta obtained by integrating (VIII) and (IX) over energy (Figure 4) with and without allowance for reactant rotation. The inclusion of the angular momentum of the reactants in the spherical approximation appears to have only a minor effect except in the low range J. It is, however, precisely in this region that the barrier for reaction 1 ascends steeply and therefore the branching ratio should vary sub-

Table II. Rotational Constants of C_4H_8 Molecules[a]

molecule	A	B	C	B^b	X^c	ref
cis-2-butene	0.536	0.171	0.136	0.152	0.536	*d*
trans-2-butene	4.8	0.110	0.108	0.109	4.8	*e*

[a] All molecules, for the purpose of the calculation, are assumed to be symmetrical tops defined by the rotational constants B and X. All constants are expressed in the dimension of cm^{-1}. [b] Degenerate rotational constant, geometric mean value. [c] Nondegenerate rotational constant. [d] T. N. Sarachman, *J. Chem. Phys.*, **49,** 3147 (1968). [e] Calculated.

Table III. Branching Ratio ($C_4H_7^+/C_3H_5^+$)

	exptl	calcd
	1. Collision	
rotationless reactants	0.11 ± 0.01[a]	0.14
rotating reactants[b]		0.11
spherical reactants		0.05
	2. Photoionization	
trans-2-butene	0.39 ± 0.03	0.42
cis-2-butene	0.38 ± 0.03	0.36

[a] References 11 and 28-31. [b] The rotational angular momentum is neglected, but its initial energy is included.

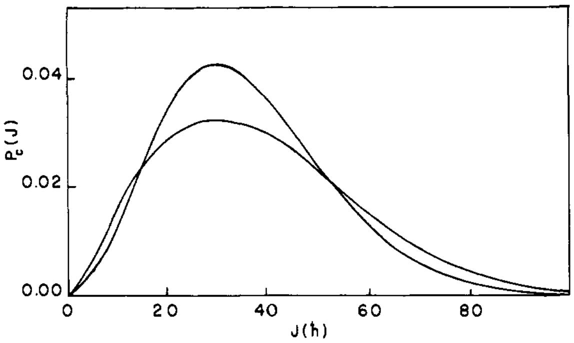

Figure 5. $P_m(J)$ for butene isomers. Identification in order of curve maxima: top, *cis*-2-butene; bottom, *trans*-2-butene.

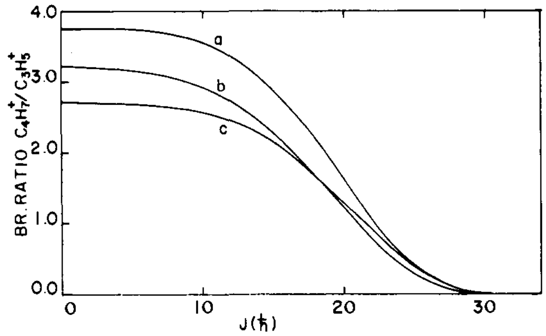

Figure 6. Variation of the branching ratio k_1/k_2 with angular momentum: (a) rotationless reactants; (b) rotational energy is available but the rotational angular momentum of the reactants is neglected; (c) the reactants are assumed to be spherical.

stantially, with a concomitant change in the overall $\langle k_1/k_2\rangle$.

B. Photoionization Process. The internal energy content of $C_4H_8^+$ prepared by photoionization is well defined when only events coincident with formation of zero kinetic energy electrons are detected. The rotational angular momentum distribution of the neutral precursor is carried over to become that of the ion after ionization since ΔJ is restricted to ±1 or zero[31] and is therefore negligible. We have assumed the C_4H_8 isomers to be symmetric tops, and used the semiclassical expression

$$P(J,K) = \frac{2B\sqrt{x/\pi}J}{(kT)^{3/2}}\exp\left(-\frac{\epsilon_r}{kT}\right)$$

$$\epsilon_r = BJ^2 + K^2(X - B) \qquad (X)$$

where K is the projection of the angular momentum J on an internal axis of the molecule, B is the rotational constant of the degenerate axis, and X is that of the nondegenerate one. The rotational constants of the relevant species are summarized in Table II. Averaging over K results in distributions much narrower than those of the collision process, and restricted to much lower values of J (Figure 5). We note here that these distributions lead one to expect, qualitatively, different kinetic energy release distributions for fragmentation of $C_4H_8^+$ prepared by photoionization and by collision as long as the transition state is loose, as observed by Klots, Mintz, and Baer.[12]

The Energy-Averaged Branching Ratio $k_1/k_2\,(J)$

It is instructive to examine the energy-averaged branching ratio to uncover which regime of angular momenta it probes with greatest sensitivity. This was investigated by examining the angular momentum dependence of the branching ratio with a fixed total internal energy of 2.57 eV as one would see it in the collision-prepared complex. Figure 6 summarizes the outcome when three different approaches are employed to treat the contribution of the molecular rotors before collision, as follows: (1) the reactants are assumed to be rotationless (i.e., 0 K rotational temperature); (2) the average rotational energy of the reactants is assumed to be available to the energy randomized in the complex, but the rotational angular momentum is neglected; (3) the reactants are approximated as spherical entities. Ethylene and ethylene ion are, of course, not spherical and option (3) may overemphasize rotational effects, while (1) neglects them entirely. All three functions exhibit similar behavior and k_1/k_2 extrapolates smoothly to zero at about 30ħ. This reflects the strong dependence of the barrier to fragmentation of reaction 1 on angular momentum. The differences between the first two reflect entirely the increase in total energy E resulting from the inclusion of the averaged rotational energy. The further lowering of $k_1/k_2\,(J)$ in the last case is a result of the coupling of J_r and L. When $J = 0$, $L = J_r$ and some low-energy collisions leading to higher values of k_1/k_2 are excluded. As J increases J_r becomes negligible with respect to L; then $J \approx L$ and the curve approaches that where $J_r = 0$ (case 1).

Comparison with Experiment

Our experimental measurement provides only total, energy, and angular momentum averaged branching ratios. In the threshold photoelectron-coincident photoion mass spectrometer, the internal energy was fixed at 2.57 eV with respect to *trans*-2-butene, which is the formal heat of reaction for formation of the collision complex.[18,19]

A number of experimental determinations of $\langle k_1/k_2\rangle$ when $C_4H_8^+$ is produced by collision have been reported.[11,32-35] Appropriate comparison requires that the reactant ethylene ion possess no excess internal energy carried over from the ionization process; there is some discrepancy, but it appears that the branching ratio at low precursor internal energy is about 0.10-0.12.

The experimental and calculated results are compared in Table III. The agreement for the ion produced by photoionization with an internal energy of 2.57 eV is good, while that for the ion produced by the collision process is best for model 2 but falls within the range of all others. We attach no significance to the better agreement with model 2; it could be argued that the molecular rotation J_r and the collisional angular momentum L do not couple effectively so that the rotational barrier is determined by the initial value of L but not by J, but there is no reasonable basis for such a statement. We believe that at this time neither the experimental reliability nor the approximations required in the calculations permit a definitive conclusion on this aspect. It is pleasing that the model we employ predicts correctly the trend and its magnitude solely on the basis of classical angular momentum considerations.

Conclusion

We conclude that angular momentum has a major effect on the outcome of ion-molecule collision processes, particularly when the exit channels include one where the fragments have low reduced mass and low polarizability. The branching ratio associated with a system such as $C_4H_8^+$ has been demonstrated to be a sensitive probe of angular momentum effects in the unimolecular fragmentation of ionic complexes.

Acknowledgments. This investigation was supported by the Department of Energy under Contract EY 76-S-02-2567; the Research Council and the University Foundation of the University of Nebraska contributed to the acquisition of equipment. Helpful discussions with Professor Bowers (University of California at Santa Barbara) are gratefully acknowledged. This report is based partly on the doctoral dissertation of G. M. L. Verboom, presented to the Graduate Faculty in partial fulfillment of the requirements for the degree of Doctor of Philosophy.

Appendix. The Joint Distribution of Energy and Angular Momentum

The method employed has already been discussed.[3] We write the differential cross section of the association reaction and normalize the expression by dividing by the Langevin capture rate. In essence we write an expression for the fraction of collisions which lead to a complex with specified E and J. The condition for complex formation is imposed by the relative magnitude of the initial relative kinetic energy ϵ_t and the barrier arising from the orbital motion and the ion-induced dipole field, that is

$$\epsilon_t > L^4/\Lambda$$
$$\Lambda = 8\alpha e^2\mu^2/\hbar^4$$

where the symbols have their usual meaning. The procedure assumes complete separation of the radial motion from the rotational motion of the reactants during the formation of the complex. Application of a previously derived formula (ref 3, eq 12) which evaluates the fraction of collisions that are determined by a maximum of the potential surface lying in excess of a particular separation of the reactants indicates that 90% of the collisions of C_2H_4 and $C_2H_4^+$ occur at separation in excess of 4.45 Å.

When rotation of the reactants is neglected, one can write the differential cross section

$$d^2k(b,v) = 2\pi v b P(v)\, db\, dv \tag{A1}$$

where b is the impact parameter, v is the relative kinetic energy, and $P(v)$ is the thermal distribution of relative velocities. Substituting $\hbar L = mvb$ and $\epsilon_t = 0.5mv^2$ one obtains

$$d^2k(L,\epsilon_t) = \sqrt{2}\pi\hbar^2(\mu kT)^{3/2}L \exp\left(-\frac{\epsilon_t}{kt}\right) dL\, d\epsilon_t \tag{A2}$$

Introducing the condition for complex formation, one can verify that

$$k_L = \int_{L=0}^{\infty} \int_{\epsilon_t = L^4/\Lambda}^{\infty} d^2k(L,\epsilon_t) \tag{A3}$$

where k_L is the Langevin rate constant. Now the fraction of collisions that lead to a complex with ϵ_t and L is just

$$P(L,\epsilon_t)\, d\epsilon_t\, dL = d^2k(L,\epsilon_t)/k_L$$
$$\epsilon_t > L^4/\Lambda \tag{A4}$$

Allowance for rotation of spherical reactants can be made by multiplying the previous expression (A4) by the rotational density of state of the reactants and a statistical factor $2J/(2L2J_r)$[36] which represents the probability of forming a state of total angular momentum J from an orbital (L) and rotational (J_r) angular momentum. The distribution $P(\epsilon_{tr},J)$ is obtained by summing all the states available at constant ϵ_{tr} and J. This can be shown to be equivalent to the method[7b] of adding up the external projection of the angular momentum and summing all states available at ϵ_{tr} and J. We have

$$P(\epsilon_{tr},J)\, d\epsilon_{tr}\, dJ$$
$$= \int_{(L)} \int_{(\epsilon_r)} \int_{(J_r)} P(L,\epsilon_t) \frac{2J}{2J_r 2L} d\epsilon_r\, dJ_r\, d\epsilon_{tr}\, dJ$$
$$\epsilon_{tr} = \epsilon_t + \epsilon_r$$
$$J = J_r + L$$

where $P(J_r,\epsilon_r)$ is the rotational density of states of the reactants. The domain of integration as well as the energy condition is identical with that of Chesnavich and Bowers (Figure 3).[7b] Two cases arise in this derivation. They correspond to the two different possible locations of L^- that are determined by the intersection of

$$\epsilon_{tr} = L^4/\Lambda + B_r J_r^2$$

and

$$J_r = J - L \text{ for } \epsilon_{tr}(J) \leqslant \epsilon_{tr} \leqslant B_r J^2$$

or

$$J_r = J + L \text{ for } B_r J^2 \leqslant \epsilon_{tr}$$

It is of interest to note that, if $P(J_r,\epsilon_r)$ is normalized, this formulation leads to a normalized distribution; otherwise one can find easily the normalization constant by integrating first with respect to energy.[37]

References and Notes

(1) Brooks and Hayes, Eds., "State to State Chemistry", ACS Symposium Series, Vol. 56, American Chemical Society, Washington, D.C., 1977.
(2) W. B. Miller, S. A. Safron, and D. R. Hershbach, *Discuss. Faraday Soc.*, **44**, 108 (1967).
(3) G. M. L. Verboom and G. G. Meisels, *J. Chem. Phys.*, **68**, 2714 (1978).
(4) H. M. Rosenstock, USAEC Report JLI-650-3-T, TID-4500 (1959).
(5) (a) P. Pechukas and J. C. Light, *J. Chem. Phys.*, **47**, 3281 (1965); (b) J. Lin and J. C. Light, *ibid.*, **43**, 3209 (1965); (c) P. Pechukas, J. C. Light, and C. Rankin, *ibid.*, **44**, 794 (1965); (d) J. C. Light, *Discuss. Faraday Soc.*, **44**, 14 (1967).
(6) (a) C. E. Klots, *J. Phys. Chem.*, **75**, 1526 (1971); (b) *J. Chem. Phys.*, **64**, 4269 (1976).
(7) (a) W. J. Chesnavich and M. T. Bowers, *J. Chem. Phys.*, **66**, 2306 (1976); (b) *J. Am. Chem. Soc.*, **98**, 8301 (1976).
(8) S. E. Buttrill, Jr., *J. Chem. Phys.*, **52**, 6174 (1970).
(9) W. N. Olmstead, M. Lev-On, D. M. Golden, and J. I. Brauman, *J. Am. Chem. Soc.*, **99**, 992 (1977).
(10) F. H. Mies, *J. Chem. Phys.*, **51**, 798 (1969).
(11) J. L. Franklin, F. H. Field, and F. W. Lampe, *J. Am. Chem. Soc.*, **78**, 5697 (1956).
(12) C. E. Klots, D. Mintz, and T. Baer, *J. Chem. Phys.*, **67**, 1636 (1977).
(13) G. Worry and R. A. Marcus, *J. Chem. Phys.*, **67**, 1636 (1977).
(14) M. L. Vestal and J. H. Futrell, *J. Chem. Phys.*, **52**, 978 (1970).

(15) E. V. Waage and B. S. Rabinovitch, *Chem. Rev.*, **70**, 377 (1970).
(16) C. F. Batten, J. Ashley Taylor, and G. G. Meisels, *J. Chem. Phys.*, **65**, 3316 (1976).
(17) C. F. Batten, J. Ashley Taylor, Bilin P. Tsai, and G. G. Meisels, *J. Chem. Phys.*, **69**, 2547 (1978).
(18) H. M. Rosenstock, U. Dray, B. W. Steiner, and J. T. Herron, *J. Phys. Chem. Ref. Data, Suppl. 1*, **6** (1977).
(19) P. Masclet, D. Grosjean, G. Mourier, and J. Dubois, *J. Electron Spectrosc. Relat. Phenom.*, **2**, 225 (1973).
(20) The error is caused by the unnormalized nature of the ratio k_1/k_2. The correct approach averages the fraction $k_1/(k_1 + k_2)$ and then obtains $\langle k_1/(k_1 + k_2)\rangle / \langle k_2/(k_1 + k_2)\rangle$. The numerical difference between the process we use and the correct one is negligible in this case. We appreciate the helpful comments of Mr. Lew Bass and Professor Michael Bowers, who pointed this out to us.
(21) (a) W. Forst, "Theory of Unimolecular Reactions", Academic Press, New York, 1973, (b) P. J. Robinson and K. A. Holbrook, "Unimolecular Reactions", Wiley-Interscience, New York, 1972.
(22) G. G. Meisels, *J. Chem. Phys.*, **42**, 2328 (1965); *Adv. Chem. Ser.*, **58**, 243 (1966).
(23) Z. Herman, Y. T. Lee, and R. Wolfgang, *J. Chem. Phys.*, **51**, 452 (1969).
(24) (a) G. G. Meisels, J. Y. Park, and B. G. Giessner, *J. Am. Chem. Soc.*, **91**, 1555 (1969); (b) *ibid.*, **92**, 254 (1970).
(25) M. S. H. Lin and A. G. Harrison, *Can. J. Chem.*, **52**, 1813 (1974).
(26) H. Budzikiewicz, C. Djerassi, and D. H. Williams, "Mass Spectrometry of Organic Compounds", Holden-Day, San Francisco, Calif., 1967.
(27) F. P.Lossing, *Can. J. Chem.*, **50**, 3973 (1972).
(28) T. Baer, D. Smith, B. P. Tsai, and A. S. Werner, *Adv. Mass Spectrom.*, **7**, (1978).
(29) M. Vestal and G. Lerner, Aerospace Research Laboratory Report 67-0114 (1967).
(30) S. W. Benson, "Thermochemical Kinetics", 2nd ed., Wiley-Interscience, New York, 1976.
(31) R. Change, "Basic Principles of Spectroscopy", McGraw-Hill, New York, 1971, p 156 ff.
(32) S. G. Lias and P. Ausloos, *J. Res. Natl. Bur. Stand.*, **75**, 589 (1971).
(33) P. Warneck, *Ber. Bunsenges. Phys. Chem.*, **76**, 421 (1972).
(34) P. R. LeBreton, A. D. Williamson, J. L. Beauchamp, and W. T. Huntress, *J. Chem. Phys.*, **62**, 1623 (1975).
(35) J. K. Kim, V. G. Anicich, and W. T. Huntress, Jr., *J. Phys. Chem.*, **81**, 1798 (1977).
(36) R. A. Marcus, *J. Chem. Phys.*, **62**, 372 (1975).
(37) G. M. L. Verboom, Doctoral Dissertation, University of Nebraska–Lincoln, Oct 1978.

Conformational Relaxation as Limitation of Chemical Models. Empirical Force Field Calculations and ^{13}C NMR Shielding Effects for Some Cyclohexanes, Bicyclo[2.2.1]heptanes, Bicyclo[3.3.1]nonane, and 11β-Substituted Estrenes[1]

Hans-Jörg Schneider,* Wolfgang Gschwendtner, and Eckehard F. Weigand

Contribution from the Fachrichtung Organische Chemie, Universität des Saarlandes, D 6600 Saarbrücken 11, West Germany.

Received May 7, 1979

Abstract: Molecular mechanics calculations on the title compounds demonstrate the redistribution of steric effects of conceptual single origin over the whole molecule. Sterically induced substituent effects on ^{13}C NMR shifts are obtained as the sum of up to ten single forces; use of nonrelaxed structures leads to gross overestimations of the interactions. A potential surface comparison between bicyclo[3.3.1]nonane and cyclohexane reveals that introduction of the bridge into cyclohexane rather extends than limits the number of conformations with similar energy in the chair inversion transition state. Considerable differences are found between published X-ray and force field derived structures of estrene derivatives, although the reflex angle between diaxial methyl groups is similar and comparable to that in isolated cyclohexanes. A potential surface calculation shows that both the C-ring distortion and the skeleton curvature brought about by axial substituents on the steroidal β side induce little strain energy variation in comparison to the binding energy to steroid hormone receptors.

In many studies of structure/energy relations and particularly of steric substituent effects, geometry variation is allowed for only in the molecule part under focus, while other parts are treated as rigid. The advent of highly efficient energy minimizing force fields[2] enables one to calculate molecular energies for any steric distortion with relaxation of *all* structural parameters. In a study of acetylcholine and derivatives, Gelin and Karplus,[3] e.g., have shown that the structural flexibility thus accessible can lead to significant variations in calculated minimum geometries and transition energies. Pursuing sterically induced substituent effects on ^{13}C NMR shifts, which are a most sensitive tool for recognition of remote steric distortions, we realized the importance of overall conformational relaxation for the observed shielding.[4] ^{13}C NMR shielding variations can be obtained by calculation of intramolecular steric forces F exerted on C–H bonds,[5] but it is necessary to localize the F contributions and to account for the redistribution of steric substituent effects with the aid of a suitable force field.[4] Because of their restricted mobility, cyclohexanes, bridged analogues, and steroids lend themselves as seemingly simple mode models for the evaluation of shielding mechanisms. The present paper is addressed to the impact of full conformational relaxation in these molecules, which contain some classical problems of conformational analysis. The structures were investigated with the Allinger MM1 force field,[2a] which provides rapid access to a large range of compounds, including hetero-substituted ones. Some recognized shortcomings of the MM1 version[6] will not alter the conclusions of the present investigation, which aims more at relative energy distributions than at accurate minima. In view of the particular sensitivity of nonbonded interactions to parametrization ambiguities we have also used an equation for the evaluation of nonbonded steric forces[4] which is based on the Lifson-Warshel force[7] field.

Substituted Cyclohexanes and Bicyclo[2.2.1]heptanes. Strain energy redistribution by relaxation is well known for axial substituted cyclohexanes, where repulsion between the substituent and 1,3-diaxial hydrogens is not solely the destabilizing factor.[5] Although numerical values dissecting the different strain contributions depend on the potential functions and parametrizations used in the force fields,[2,6] it is not disputable that the gauche hydrogen effect between the equatorial hydrogen at Cα (H8 in **1**) and the equatorial hydrogen at Cβ (H9 in **1**) can be a significant factor destabilizing the conformer

0002-7863/79/1501-7195$01.00/0